

Biochemical and rheological analysis of human colonic culture mucus reveals similarity to gut mucus

R. Logan Howard,^{1,2} Matthew Markovetz,^{1,2} Yuli Wang,³ Camille Ehre,^{1,4} Shehzad Z. Sheikh,⁵ Nancy L. Allbritton,³ and David B. Hill^{1,2,*}

¹Marsico Lung Institute, University of North Carolina at Chapel Hill, Chapel Hill, North Carolina; ²Department of Physics and Astronomy, University of North Carolina at Chapel Hill, Chapel Hill, North Carolina; ³Department of Bioengineering, University of Washington, Seattle, Washington; ⁴Division of Pediatric Pulmonology, The University of North Carolina at Chapel Hill, Chapel Hill, North Carolina; and ⁵Division of Gastroenterology and Hepatology, University of North Carolina School of Medicine, Chapel Hill, North Carolina

ABSTRACT The goal of this project was to validate the functional relevance and utility of mucus produced by an in vitro intestinal cell culture model. This is facilitated by the need to physiologically replicate both healthy and abnormal mucus conditions from native intestinal tissue, where mucus properties have been connected to intestinal disease models. Mucus harvested from colonic cell cultures derived from healthy donors was compared to mucus collected from surgically resected, noninflamed transverse colon tissue. The rheological and biochemical properties of these mucus samples were compared using oscillational rheometry, particle-tracking microrheology, multiangle laser light scattering, refractometry, and immunohistochemical imaging. An air-liquid interface culture of primary human colonic epithelial cells generated a continuous monolayer with an attached mucus layer that displayed increasing weight percent (wt%) of solids over 1 week ($1.3 \pm 0.5\%$ at 2 days vs. $2.4 \pm 0.3\%$ at 7 days). The full range of mucus concentrations (0.9–3.3%) observed during culture was comparable to that displayed by ex vivo mucus (1.3–1.9%). Bulk rheological measurements displayed similar wt%-based complex viscosities between in vitro and ex vivo mucus, with the complex viscosity of both systems increasing with wt% of solids. Particle-tracking microrheology showed higher complex viscosities for ex vivo mucus samples than in vitro mucus which was explained by a greater fraction of water present in in vitro mucus than ex vivo, i.e., in vitro mucus is more heterogeneous than ex vivo. Refractometry, multiangle laser light scattering, and immunostaining showed increased mucus complex size in ex vivo mucus compared with in vitro mucus, which may have been due to the admixture of mucus and cellular debris during ex vivo mucus collection. The air-liquid interface culture system produced intestinal mucus with similar composition and rheology to native human gut mucus, providing a platform to analyze pathological differences in intestinal mucus.

SIGNIFICANCE Our work is motivated by the need to establish in vitro systems that accurately mimic gut mucosa. Herein, we describe an air-liquid interface gut cell culture system that produces a mucus layer which is similar to ex vivo gut mucus. The novelty of this system lies in the formation of an intact mucus layer which, over time, will accumulate sufficient mucus to allow for rigorous characterization. The rheological and biochemical properties of this mucus were measured and compared to native gut mucus, showing similarity in mechanical properties such as viscosity but differences in structural composition.

INTRODUCTION AND BACKGROUND

Mucus in the gastrointestinal (GI) tract is produced in the luminal tissue layer known as the mucosa, which is primarily composed of an epithelial layer of cells on top of a loose

layer of connective tissue, the lamina propria. A healthy GI mucus layer is critical for protection from pathogens, cell signaling, and lubrication of solid waste passing through the intestines (1). Mucus is a hydrogel composed of inorganic salts, enzymes, and proteins, as well as large molecular weight mucin glycoproteins (2). Mucins give mucus its characteristic viscoelastic properties and are primarily produced by goblet cells within the digestive system (3). Mucin glycoproteins consist of nearly 80% carbohydrates bound to a protein backbone (4,5). Mucus in the gut removes bacteria

Submitted February 26, 2021, and accepted for publication October 19, 2021.

*Correspondence: dbhill@med.unc.edu

Editor: Paul Janmey.

<https://doi.org/10.1016/j.bpj.2021.10.024>

© 2021 Biophysical Society.

This is an open access article under the CC BY-NC-ND license (<http://creativecommons.org/licenses/by-nc-nd/4.0/>).

and debris due to fluid flow from intestinal peristalsis, necessitating mucus secretion to replenish the layer (6). Mucus clearance times have been observed to be as rapid as 1 h in the gut, indicating that constant secretion is essential to maintaining a healthy mucus protection in the GI tract (6).

Mucus in the GI tract can be organized as either a single layer of loose, gel-like mucus (e.g., small intestine), or a two-layer system with a loosely-packed outer layer and a more compact inner layer against the epithelial cell wall (e.g., stomach, large intestine) (7–9). Colonic mucus is predominantly composed of MUC2, which has a monomeric weight of ~ 2.5 MDa (10). Mucins in gut mucus are organized into a gel network that provides a supporting structure for the intestinal mucus layers (10). The inner layer of colonic mucus has a height of ~ 100 μm , is tightly packed, and is devoid of bacteria in healthy patients (11). At the luminal edge of the inner layer of mucus, the mucus complex transitions from a tightly packed layer into a loose, larger network that is hundreds of microns thick and is stabilized by disulfide bonds between cysteine residues on mucins (12). The outer mucus layer may be penetrated by bacteria, debris, and fecal matter, and must undergo regular clearance due to fecal pressure and fluid flow within the colon (12). These two distinct layers are generally observed in healthy patients with normal levels of colonic content and microbiota, but can present altered phenotypes in abnormal conditions (13). The transition from inner to outer layer mucus is poorly characterized, but is hypothesized to be driven by proteolytic cleavage (12). In total, healthy gut mucus facilitates pathogen and debris removal from the GI tract, and its viscoelastic properties are largely determined by mucin interactions.

Representative *in vitro* models of gut mucus are difficult to design and maintain. The large intestine displays a unique and complex native physical structure, characterized by the presence of ~ 400 - μm cylindrical cavities embedded in the epithelial wall known as “intestinal crypts.” The crypts display a polarization between stem cells at the basal level of the crypt and differentiated cells closer to the epithelial lumen (14). Crypt polarization is primarily driven by chemical gradients from the base of the crypt, which are partially responsible for driving cell proliferation and differentiation (15). Goblet cells, which produce mucus, can be found along the inner ring of these crypts closer to the lumen, and serve as anchor points for the inner layer of intestinal mucus (12). *In vivo* tissue displays a complex balance between commensal microbiota growth in the outer layer of mucus, including their associated metabolite production, and protection in the inner layer of mucus from pathogenic bacteria (16). It has recently been demonstrated that a two-tiered gut mucus layer with physiologically relevant thickness is obtainable *in vitro* (16,17); however, the rheological and biochemical properties of *in vitro* gut mucus remain poorly characterized (16,17).

There are fundamental challenges in effectively recapitulating a contiguous mucus layer using *in vitro* tissue culture. The chemical composition of native mucus is difficult to replicate, as the entire mucus layer is composed of variable amounts of mucins, lipids, and other proteins (18). Similarly, the group of metabolic factors responsible for instigating mucus secretion is not fully understood. For example, vasoactive intestinal peptide (VIP) has been demonstrated to stimulate goblet cell growth and mucus production but is not commonly included in cell culture media (19). It has also been shown that exposure of the mucus layer to various pathogens *in vivo* causes alterations in mucus properties, which is difficult to replicate *in vitro* without a significant decrease in cell viability (18). Finally, with typical aseptic cell culture techniques, the epithelial cell layer is regularly washed and aspirated, making it difficult for a continuous mucus layer to be maintained across the surface of the cells due to regular convective mixing (20,21).

To combat these shortcomings, we systematically characterize mucus produced by air-liquid interface (ALI) culture (21). In this system, human primary colonic epithelial cells are grown to confluence on a microporous membrane with media containing VIP in a basal reservoir beneath the cells. Mucus secreted by the cells accumulates in the luminal compartment (21,22), which is then collected for biochemical and biophysical characterization and compared to mucus isolated from healthy patients. Although this method does not possess a biomimetic microstructure (monolayer versus crypts) or peristaltic fluid flow, the system provides a thick, contiguous mucus layer after 2–3 days of culture (21–23). Herein, we demonstrate that the ALI colonic cell culture system generates and maintains a mucus layer that replicates the composition, structure, and physical properties of native colonic mucus.

MATERIALS AND METHODS

ALI culture of intestinal epithelial cells

Cells derived from human transverse colon samples were cultured and expanded as described in previous publications (16,21,23). Cells were acquired from colonoscopies at the University of North Carolina’s Hospital Meadowmont Endoscopy Center (Chapel Hill, NC) with informed consent of the patient (under the approved University of North Carolina Institutional Review Board #14-2013) and were collected from three separate donors (age 50, male; age 65, female; age 12, male). All experiments in this study were conducted using cells between passage 5 and 10 (P5 and P10). Cells demonstrated a normal karyotype through P11 (23). A solution of 1% Matrigel (Fisher Scientific, Fremont, CA) in cold $1\times$ phosphate-buffered saline (PBS) was prepared. 1 mL each of this solution was placed in the top compartment of 12-well polyurethane transwell inserts with 0.4 μm pores (#3460; Corning, Corning, NY). After insertion, these transwells were incubated for 24 h at 37°C, then rinsed twice with sterile $1\times$ PBS. Transverse cells were then plated in these transwell inserts in expansion medium described in previous publications (16,23). 1 mL of expansion medium containing cells was placed in the top compartment of each transwell, and 2 mL of expansion medium without cells was placed in the bottom compartment underneath each transwell. Media were changed at 3 days. At 5 days, a solution of

differentiation media (described previously in (16,23)) with 330 ng/mL VIP (#AS-22872; AnaSpec, Fremont, CA) was prepared. 0.5 mL of this media was added to the basal compartment beneath each transwell and replaced every 24 h. This left the apical surface of the cells exposed as an ALI. Cells were cultured for 2–7 days in these conditions, with samples collected from each day and stored separately. For mucus collection, a positive pressure pipette was used to collect and store the viscous mucus samples.

Mucus harvest from ex vivo surgical resections of intestinal tissue

Ex vivo surgical resections from human colonic biopsies were received in Roswell Park Memorial Institute 1640 growth medium from the Shehzad Sheikh Laboratory (Division of Gastroenterology and Hepatology, University of North Carolina at Chapel Hill). These samples were acquired from colonoscopies at the University of North Carolina's Hospital with informed consent of the patient (under the approved University of North Carolina Institutional Review Board #10-0355). Samples were collected from five patients, all from noninflamed transverse colon tissue (age 45, male; age 52, male; age 38, female; age 26, male; age 61, female). These samples were transported and harvested for mucus within 2 h of receipt. All samples were initially weighed, and their patient code recorded and placed within a p100 petri dish (Fisher Scientific, Fremont, CA). Initially, a spatula was used to scrape off the visible mucosa layer from the epithelial side of the samples, and this scraping was collected in a 15-mL tube. The samples were then incubated for 10 min in the petri dish on a rotary platform at 37°C with 1 mL of 1 × PBS per gram of sample. This wash was collected and stored in a separate 15-mL tube. These samples were then frozen at –20°C until needed for analysis.

Macrorheology for mucus analysis

Bulk rheological properties of the mucus samples were measured using cone-and-plate oscillational rheometry (20 mm cone, 1° deflection). 40 μL of each sample were loaded onto the bottom Peltier plate of a DHR-3 rheometer (TA Instruments, New Castle, DE). Next, two separate steps of oscillatory shear testing were conducted. First, the linear viscoelastic region (LVR) for the storage modulus (G') and the loss modulus (G'') was determined by applying a range of small strains to each sample (0.01–10%) at two frequencies (1 and 5 Hz). Next, a frequency sweep of a constant strain magnitude (1%) were applied to the same sample from 0.1 to 100 Hz, generating a frequency versus modulus plot for G' , G'' , and the complex viscosity (η^*). Mechanical sweeps were conducted with three separate loads from each sample to account for variance.

Microrheology for mucus analysis via microparticle tracking

For rheological properties on the microscale, 30 μL of each mucus sample was aliquoted into a separate conical tube. After this, each sample was loaded with 0.5 μL of 1-μm diameter fluorescent carboxylated beads (F8823; Thermo Fisher Scientific, Fremont, CA) and left for 24 h at 4°C on a rotating platform to allow beads to mix into the samples. After this, 5 μL of each sample was placed on a glass slide underneath a glass coverslip. Using a Nikon Eclipse TE2000U microscope (Nikon Instruments, Melville NY) with a 40× air objective (NA = 0.95), the motion of the beads was recorded at 60 frames per second for 30 s. The movement of each bead was automatically tracked using a custom Python program, TrackPy (<https://doi-org.libproxy.lib.unc.edu/10.5281/zenodo.34028>). The mean squared displacement and complex viscosity (η^*) values were calculated for each bead in accordance with mathematics described previously, primarily based on the Stokes-Einstein equation (24,25). Values of complex viscosity, mean-square displacement, and diffusion coefficient could be calculated from the following equations:

$$\eta^*(\omega) = \frac{(G'^2 + G''^2)^{1/2}}{\omega}, \quad (1)$$

$$MSD(t) = 4Dt, \quad (2)$$

and

$$D = \frac{k_b T}{3\pi\eta^* d}, \quad (3)$$

where k_b is the Boltzmann constant, D is the diffusion coefficient, T is temperature, t is time, and d is the diameter of the particle being used. It should be noted that η^* in this equation is frequency dependent when measured in viscoelastic fluids, and can be derived by applying a Fourier transform to the measured shear modulus (26).

Biochemical mucus analysis

By measuring the scattering angle and intensity of a laser-illuminated mucus sample, biochemical properties such as molecular weight, total sample mass, and radius of gyration were determined. 10 μL of the mucus samples were mixed as a 20% solution in 6 M GuHCL at 25°C for 20 min, to break non-covalent bonds leaving large mucin protein complexes. These samples were then diluted further at a ratio of 1:10 or 1:40 in light scattering buffer (pH 7.0). Proteins and mucins in this solution were then separated using high-pressure liquid chromatography (CL2B column). Light scattering was performed using the Optilab t-REX refractometer (Wyatt Technology, Santa Barbara, CA) and Dawn Heleos II multiangle laser photometer (Wyatt Technology).

Immunohistochemical staining and imaging

Mucus samples (both scrapings and apical washings) were pipetted onto positively charged microscope slides and dried at 25°C for 1 h. The samples were then fixed with 10% neutral buffered formalin for 5 min and washed with 1 × PBS three times for 5 min and then blocked with 3% bovine serum albumin (BSA) in 1 × PBS for 1 h at 25°C. After blocking, the 3% BSA solution was replaced with a primary antibody solution of MUC2 antibody (Mouse Anti-Human MUC2; BD Biosciences, San Jose, CA). This primary antibody was diluted 1:1000 in 3% BSA solution. After incubating 16 h at 4°C, protected from light and kept moist using wet paper towels in a slide box, the samples were washed three times with 1 × PBS for 5 min each and incubated in secondary antibody solution at 25°C for 1 h. The secondary antibody solution was composed of Alexa Fluor 594 donkey anti-mouse IgG (mouse red, Fisher Scientific, Fremont, CA), diluted 1:1000 in 3% BSA solution. After 1 h, the secondary antibody solution was replaced with 4',6-diamidino-2-phenylindole (DAPI) diluted 1:1000 in 1 × PBS for 5 min at 25°C. The samples were then washed with 1 × PBS three times for 5 min each, aspirated, and the slides were mounted using FluorSave (Sigma-Aldrich, St. Louis, MO) mounting oil and 24 × 50 mm, #1.5 coverslips and sealed with clear nail polish. The samples were imaged using the Olympus VS120 virtual microscope (slide scanner) and the Olympus Fluoview FV1000 (confocal) microscope (Olympus Microscopy, Shinjuku, Japan). For quantification, MATLAB R2019b (The MathWorks, Natick, MA) was used to outline individual mucus complexes using pixel thresholding and calculate their size.

Weight percent solids measurements

50–100 μL of mucus was aliquoted on a preweighted foil square and the combined mass of the mucus sample and foil square was measured. The sample and foil were incubated for 16 h at 80°C. The final mass of the

sample and foil were measured, followed by calculation of the percent solids remaining after liquid evaporation.

Transepithelial electrical resistance measurements

Using the cell culture technique described above, cells were cultured on three transwell inserts to confluence and then cultured under the ALI + VIP for 5 days to accumulate mucus. The apical and basal reservoirs of these inserts were washed two times with $1 \times$ PBS. Additionally, a transwell insert without any cells was washed two times with $1 \times$ PBS. The transepithelial electrical resistance (TEER) of each insert was measured using a Millicell ERS-2 Voltohmmeter (MilliporeSigma, Burlington, MA). This measurement was conducted three times per well, with the probe placed at different locations within each well for each measurement.

pH measurement of apical and basal reservoirs of transwell inserts

Using the cell culture technique described above, cells were cultured on nine transwell inserts to confluence and then cultured under the ALI + VIP for 5 days to accumulate mucus. pH was measured using a Mettler Toledo S220 SevenCompact Benchtop pH/ISE Meter (Mettler Toledo, Columbus, OH) at 25°C. The pH was measured in the basal and luminal reservoir within a time span of 3 min. To control for temperature-dependent changes in pH, the pH of the basal reservoir was tested again directly after testing of the apical reservoir.

Statistics

To determine statistical significance, two-tailed, two-mean *t*-tests were conducted using the mean and standard deviation of each variable of interest and comparing between in vitro and ex vivo sample data. Statistical significance was defined using 95% confidence intervals, with *p* values < 0.05. For power-law analysis, power-law equations were fit to gathered data using OriginPro 2020 (OriginLab, Northampton, MA).

RESULTS AND DISCUSSION

Characterization of mucus generation and collection

Our primary objective was to establish whether the ALI culture system of colonic epithelial cells could generate a physiologically relevant in vitro colonic mucus (Fig. 1). Human colonic epithelial cells were cultured to confluence (5 days in expansion medium rich in growth factors) followed by removal of this medium and replacement with differentiation media (devoid of growth factors) containing VIP (21). Mucus accumulated in the luminal reservoir for 2–7 days and was then harvested and used in biochemical and biophysical characterization assays. The integrity of the monolayer beneath the accumulating mucus was characterized by measurement of the TEER (Fig. 2 a). Cultures were grown in triplicate for 10 days (5 days in an expansion, 5 days cultured at ALI + VIP) for TEER measurements. A blank transwell containing no cells was prepared as a control. Colonic monolayers exhibited a statistically significantly ($p < 0.05$) greater resistance compared with that of the con-

trol. The measured monolayer resistance of 364–422 $\Omega \cdot \text{cm}^2$ is similar to that predicted for in vivo colonic epithelium (27). Thus, this in vitro system was successful at generating a contiguous monolayer of colonic epithelial cells.

It must be acknowledged that there are a few potential drawbacks to this ALI culture system and the comparative analysis with ex vivo mucus scrapings. This is a monolayer system rather than a physiological crypt system, so mucus generation and anchoring may be affected. It is also a sterile in vitro system, so mucus interactions and behavior related to both bacteria and antimicrobial peptides are likely absent. Finally, regarding the ex vivo samples, the collection process could prove disruptive to the native mucus structure and properties. Although these limitations must be considered, the data presented in this section regarding the presence and collectable volume of mucus gives evidence that the ALI culture system can prove useful for initial analyses of the properties of native versus in vitro gut mucus.

The concentration of the mucus layer produced by the cultures, as measured by percent solids dry weight, was hypothesized to increase as a function of the time the mucus layer was allowed to accumulate. To test this hypothesis, mucus from cultures was harvested after 2–7 days of accumulation, and the concentration of solids was measured using the dry weight method (22). Human colonic cells from donors of both genders and ages ranging from 12 to 65 were used. The percentage of solids significantly increased with the number of culture days (Fig. 2 b), with $2.4 \pm 0.3\%$ after 7 days of accumulation and $1.3 \pm 0.5\%$ after 2 days ($p = 0.029$). Percentage of solids has been established as a marker of mucus concentration when cells are grown in an ALI culture system, due to secreted mucins not being removed and thus being allowed to accumulate on the apical side of the culture (22). We take advantage of this marker to connect an increased percentage of solids with increased mucus accumulation. These data also coincide with data collected in Wang et al. 2019 (21), showing increased mucus accumulation over time on ALI culture. Thus, it was established that longer duration of culture with ALI + VIP supported continuous mucus secretion and accumulation, and supported collection of large volumes (200–300 mL, on average) of mucus. This level of mucus was useful for conventional rheological and biochemical testing of in vitro mucus as a function of solids concentration.

One unexpected phenomenon was that the pH of the mucus layer and luminal fluid was more basic than that of the basal media after 5 days of mucus accumulation ($p < 0.05$), with pH values measured in the apical and basal reservoirs in nine transwells (Fig. 2 c). The increased alkalinity was likely due to secretion of basic compounds (e.g., sodium bicarbonate) through cell-based ion channels into the luminal reservoir (28). These data suggest that it may be advantageous for the gut to produce an alkaline mucus layer to protect the underlying cells from acidic conditions, which has been observed in native mucus (28). Future studies are

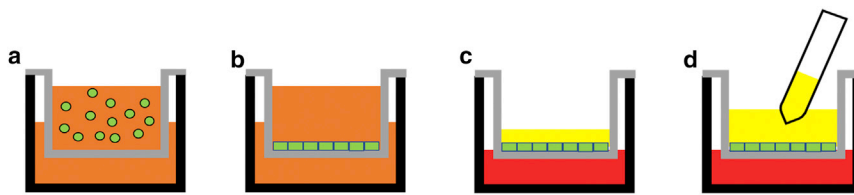


FIGURE 1 Schematic of ALI + VIP culture of colonic cells followed by mucus collection. (a) Cells (green) are seeded on a microporous insert (gray) with expansion medium (orange) in both the apical and basal reservoirs. (b) Cells are grown into a confluent monolayer over the course of 3–5 days. (c) After confluence is achieved, both the apical and basal media are aspirated. Differentiation medium with VIP (red) is placed in the basal reservoir underneath the microporous insert. No medium is added to the apical reservoir. A hydrated continuous mucus layer (yellow) forms on the surface of the epithelial cells. (d) After 2–7 days of culture, the mucus layer is collected.

reservoir underneath the microporous insert. No medium is added to the apical reservoir. A hydrated continuous mucus layer (yellow) forms on the surface of the epithelial cells. (d) After 2–7 days of culture, the mucus layer is collected.

needed to determine which ion channels are being activated during culture with an ALI. Our system would also allow for monitoring of daily pH changes with regards to variables of interest within the colon, such as infection, CO₂ concentration, etc.

Macrorheological analysis of intestinal mucus using oscillational rheometry

Bulk rheological properties of *in vitro* and *ex vivo* mucus (storage modulus, G' ; loss modulus G'' ; and complex viscosity, η^*) were characterized using cone-and-plate oscillational rheometry. We hypothesized that higher percentage solids would correlate with increased mechanical properties in mucus. Additionally, we hypothesized that *ex vivo* samples would display greater viscoelastic moduli than *in vitro* samples due to exposure to intestinal bacteria in native conditions, facilitating more interactions within the mucus network and increasing mucus's rheological properties. Whether these increased interactions arise from oxidation (29), inflammation (30), pH (31), or other factors remains to be determined. First, an amplitude sweep of increasing strain rates was conducted at two constant frequencies, 1 and 5 Hz, representative of native *in vivo* intestinal contraction rates to determine the LVR as previously described (16). The LVR represents a range of strains, or deformations, where a viscoelastic material displays rheological properties that behave independently of the applied strain, allowing for comparison between samples without

accounting for the nonlinear properties of mucus (32). A strain of 1% was applied in a frequency sweep to determine macroscopic storage modulus, G' and loss modulus, G'' , as this strain fell within the LVR for both *in vitro* and *ex vivo* samples. Storage and loss moduli were then evaluated as a function of the concentration of solids (Fig. 3, *a* and *b*).

For all samples, G' was greater than G'' (Fig. 3 *c*), indicating an elastic-dominant effect called gelation (16). Of note, the ratio of G'/G'' did not change as a function of percent solids for the *in vitro* samples. The *ex vivo* mucus displayed larger G' and smaller G'' values than *in vitro* samples at similar concentrations, suggesting that *ex vivo* samples are more solid-like than *in vitro* samples. The elastic-dominant effect is likely due to the increased presence of cells and other debris trapped in the *ex vivo* mucus samples, where the foreign matter acts as a cross-linker of the mucus network. As expected, the rheological properties of both *in vitro* and *ex vivo* mucus samples were positively correlated with percent solids. For *in vitro* samples, these correlations were statistically significant ($p \lll 0.01$), which agrees with the literature of power-law scaling below a threshold concentration of mucins/solids (33–35). Here, our samples displayed power-law correlations of $G' \sim c^{0.1595}$ and $G'' \sim c^{1.599}$. The *ex vivo* samples similarly displayed a concentration-dependent increase in both G' ($\sim c^{0.802}$) and G'' ($\sim c^{1.916}$), but did not display as strong of a power-law correlation, with p values of 0.222 and 0.154, respectively. It is important to note that, because of the small range of concentrations, it is possible a power-law

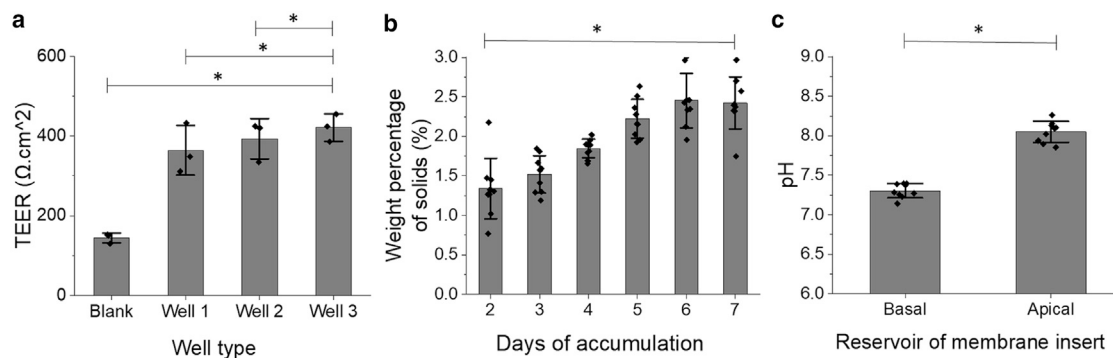


FIGURE 2 Properties of the VIP + ALI epithelial monolayers. (a) TEER was measured across confluent layers of colonic epithelial cells ($n = 3$), cultured on microporous inserts. Additionally, a microporous insert with no cells (submerged in PBS) was measured as a control. (b) Mucus was collected from monolayers ($n = 3$ per day) over 2–7 days and the weight percentage of solids was measured. (c) The pH of the apical and basal reservoirs of cell monolayers was measured ($n = 9$). $*p < 0.05$.

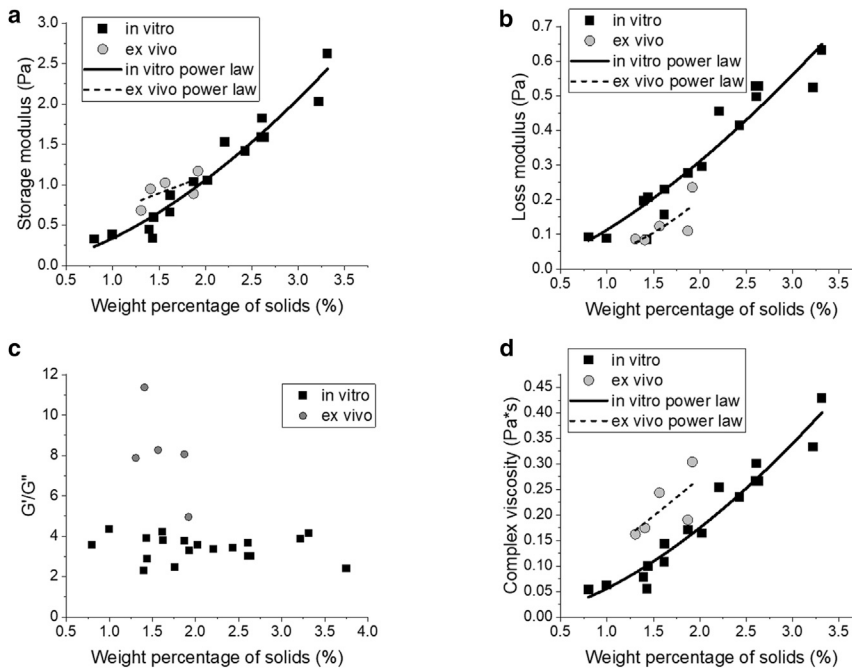


FIGURE 3 Bulk rheology of mucus samples. In vitro mucus samples grown from three separate transverse colon donors were collected from 2 to 7 days for each sample. Similarly, ex vivo mucus samples were collected from five separate samples of surgical resection tissue from noninflamed transverse colons. These samples were measured in 40 μL aliquots using cone-and-plate oscillational rheometry, measuring the storage modulus (a) and loss modulus (b) of the mucus. To demonstrate gelation, which is indicated when $G' > G''$, G'/G'' was plotted for each sample (c). The complex viscosity at 1 Hz was calculated and plotted for each sample against the weight percentage of solids (d). Power laws are plotted for both in vitro and ex vivo data for (a), (b), and (d).

correlation would not remain at concentrations outside of this range (between 0 and 1% solids, and above $\sim 2.5\%$ solids). However, the collected ex vivo samples demonstrated a tight grouping of concentrations, and the in vitro samples had a similar (though slightly larger) grouping; this would indicate that a power-law concentration can be observed in physiologically relevant concentration ranges at this time.

The combined magnitude of the viscoelastic moduli of a hydrogel can be expressed as one variable, the complex viscosity (η^*) via Eq. 1 (Materials and methods) (36). Samples were analyzed at 1 Hz due to its physiological relevance (i.e., intestinal contraction rates) (16). The complex viscosities of both sample types were plotted as a function of their concentration of solids (Fig. 3 d). Similar trends were observed for η^* as were measured in G' and G'' . The in vitro samples displayed a strong concentration-dependent power-law correlation ($\eta^* \sim c^{1.492}$, $p \lll 0.01$) and the ex vivo samples displayed a more modest correlation ($\eta^* \sim c^{2.082}$, $p = 0.199$). Additionally, ex vivo samples exhibited more robust mechanical properties than in vitro samples with comparable concentrations of solids.

Particle tracking microrheology of in vitro and ex vivo gut mucus

Although microrheology yields a robust characterization of the bulk properties of mucus that are associated with clearance, particle tracking microrheology (PTMR) is able to characterize mucus on a length scale that is associated with pathogen motility (37,38). Additionally, unlike microrheology, PTMR is able to analyze the inherent heterogeneity

of mucus (39,40). Using these advantages of PTMR, multiple individual slide samples ($n > 50$ for in vitro mucus, $n > 15$ for ex vivo mucus) with a range of mucus concentrations from ~ 1 to 4% solids were incubated with beads, recorded over time via microscopy, and tracked via PTMR to generate rheological data. Consistent with our previous observations (25,41,42), greater mucus concentrations are associated with decreased particle mobility (Fig. 4 a). 1- μm beads in 1.2% mucus are able to traverse a much greater area than a similar bead in 3.2% mucus.

Converting particle mobility into rheological properties via the generalized Stokes-Einstein relationship (see Materials and methods), PTMR confirms our earlier observation (Fig. 3 d) that the complex viscosity (η^*) of ex vivo mucus is greater than that of in vitro mucus at similar concentrations (~ 1 –2% solids; Fig. 4 b). The mean viscosity at 1 Hz of ex vivo mucus samples was greater than that of in vitro samples, 0.42 ± 0.59 and 0.02 ± 0.20 Pas, respectively. Although not statistically significant ($p = 0.169$), this trend suggests that the ex vivo samples have a slightly stiffer underlying matrix compared to the in vitro counterparts. It should also be noted that the large variance in the ex vivo samples agrees with the hypothesis that the native mucus samples form more heterogeneous complexes. As with our macroscopic results, we speculate the increased viscosity in ex vivo mucus arises from intramucus interactions resulting from oxidation (29), inflammation (30), pH (31), or other factors.

To ascertain the degree of heterogeneity of the mucus samples, we applied Gaussian mixture modeling to the distributions of η^* measured at 1 Hz for both ex vivo and in vitro specimens (Fig. 4 c). This method has been

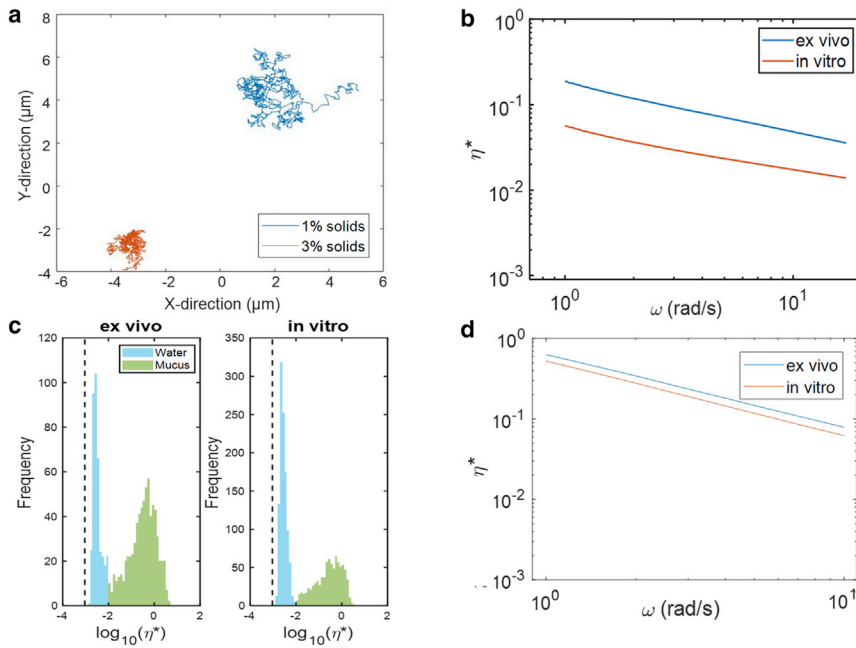


FIGURE 4 Mucus microrheology via microbead tracking. Collected mucus samples from both in vitro and ex vivo donors were tested for weight percentage of solids, and samples within the range of 1.4–2.0% solids were separated into 40 μL aliquots. These aliquots were loaded with fluorescent beads, and the movement of these beads was tracked for 30 s, with 30 videos/image sequences per sample. (a) Representative trajectories of individual beads from in vitro mucus comprised of 1% solids and 3% solids were tracked and plotted in the x - y plane. (b) Complex viscosities were calculated from the average MSD of all beads in the in vitro and ex vivo mucus samples. These viscosity measurements record average η of individual tracked beads for a given ω , across all videos tracked via PTMR for a given sample. (c) The log of the complex viscosity at 1 Hz of each individual bead in each set of samples was calculated, and these values were plotted based on their frequency of occurrence. These histograms displayed two distinct peaks, one close to the viscosity of water, and the other representing beads stuck in mucus complexes via our PTMR tracking software. (d) The frequency-dependent range of complex viscosities was calculated and plotted only for beads embedded in a mucus complex.

demonstrated to effectively categorize beads that are either trapped in mucus or effectively free-floating in water using PTMR (40). The in vitro samples displayed a greater overall percentage of beads in water (55%) compared with beads in water (blue peak) in the ex vivo samples (29%), which suggests that cultured samples may accumulate less mucus than is present ex vivo. The second peak (green) found in the 10^{-2} – 10^{-1} Pa \cdot s range was measured by beads within the mucus gel. Analysis of beads from these secondary peaks alone shows the ex vivo samples exhibited an average viscosity of 0.28 ± 0.61 Pa \cdot s, whereas the in vitro samples had an average viscosity of 0.24 ± 0.16 Pa \cdot s at 1 Hz. These data suggest that the mucus components of the samples displayed statistically indistinguishable ($p = 0.85$) microrheological properties. The η^* of beads in the mucus gel was tracked over a range of angular frequencies (Fig. 4 d). The observed trends gave evidence that the ex vivo samples were more heterogeneous mucus complexes, whereas the in vitro samples indicate a more diffuse mucus layer with a lower degree of heterogeneity. However, these observations also show that although the mucus may form different types of complexes in ex vivo and in vitro samples, they display similar rheological properties on the microscale. Thus, in vitro gut mucus cultured at ALI is a potential model for native gut mucus and exhibits physiologically relevant biophysical properties.

Biochemical characterization of mucins

It is essential for in vitro mucus model systems to replicate both the rheological and biochemical properties of native

mucus. We therefore characterized the mass, molecular weight, and radius of gyration of mucins in each mucus type using size-exclusion chromatography with multiangle laser light-scattering and refractometry. The data represented in this article were collected from diluted, but not intentionally denatured (i.e., with DTT or GuHCL), mucus samples. The first notable difference observed between the samples was found in their total mass of mucins (Fig. 5 a), where a significantly greater mass of covalently-bound complexes was measured in the ex vivo samples compared with in vitro ($p = 0.013$). Further biochemical characterization demonstrated differences in mucus phenotypes between the mucus samples, particularly in the average molar mass of the analyzed mucus complexes (Fig. 5 b). Ex vivo samples exhibited a statistically significant greater ($p < 0.001$) molar mass ($2.6 \times 10^3 \pm 8.1 \times 10^2$ MDa) compared with the in vitro molar mass ($6.9 \times 10^2 \pm 4.6 \times 10^2$ MDa). This ~4-fold increase in molar mass would suggest that larger mucin complexes are produced in native tissue, whereas the in vitro samples produce a looser, more diffuse layer of mucus. This hypothesis is further supported by the average radii of gyration of mucins (Fig. 5 c) from the two samples where mucins from the ex vivo samples displayed a statistically larger radius of gyration compared to the in vitro samples ($p = 0.018$). The presence of additional debris in the ex vivo samples could contribute to this phenomenon and allow for mucus network nucleation rather than primary mucin complex bonding. It is likely that the overall size of the mucin polymers is smaller in vitro due to differences in growth conditions. These theories will be further evaluated using a stronger dilution liquid and with analysis via SDS

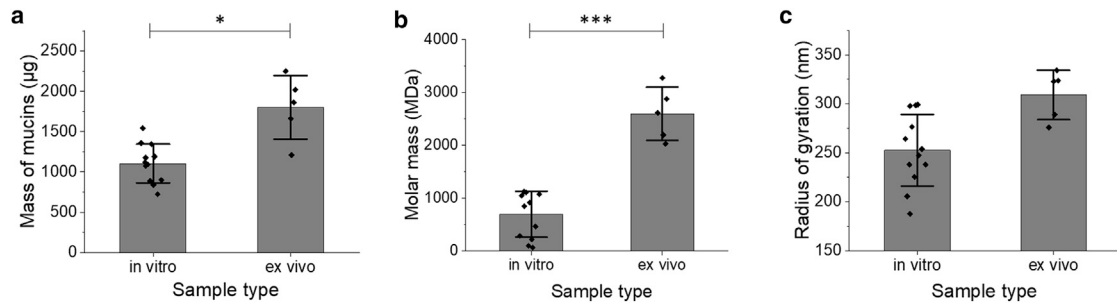


FIGURE 5 Biochemical properties of mucus samples via size-exclusion chromatography with multiangle laser light-scattering and refractometry (SEC-MALS). Mucus was separated by size exclusion chromatography and detected by multiangle light scattering, measuring the total mass of mucins in the sample (a), average molar mass (b), and average radius of gyration (c). * $p < 0.05$; *** $p < 0.001$.

(sodium dodecyl sulphate) gel electrophoresis to characterize the mucin molar mass heterogeneity within the samples.

Staining and analysis of in vitro and ex vivo mucus samples

To further characterize mucus samples, collected samples were immunostained and imaged using confocal microscopy. Using an anti-MUC2 antibody for intestinal mucus (red) and DAPI for DNA (blue), both in vitro and ex vivo mucus were immunolabeled and imaged via confocal microscopy (Fig. 6). Compared with the ex vivo samples, DNA signal was minimally detected in the in vitro samples, suggesting that fewer cells shed into the apical cell washings than cells detaching from biospecimens. In addition, DNA signal in the ex vivo samples revealed the presence of clumps of cells that colocalized with mucus, indicating that the epithelial cell layer was scraped during collection. By contrast, in vitro mucus collection by washing is a gentler process. It is important to note that the minimal presence of DNA/cells in the in vitro mucus samples leads us to believe that cell-binding minimally influenced rheological properties of the collected mucus. Mucus staining provides evidence that ex vivo mucus tends to form larger complexes, whereas the organization of in vitro mucus is looser in appearance. Likely, the larger complexes observed in ex vivo samples are caused by the physical scraping of the submucosa during surgical collection.

After staining, the differences in mucus complex size and coverage were quantified between the two sample types. Using MATLAB, the outline of each individual mucus complex in each image was determined (Fig. 7, a and b). To provide quantitative analysis, these images with outlined mucus complexes had background fluorescence subtracted, to allow for image-to-image comparison. These images were then used to calculate the average size of a mucus complex (Fig. 7 c) and the overall surface coverage of mucus (Fig. 7 d) for each sample type. Although only the average mucus complex size yielded statistically significant results ($p < 0.05$), the overall trends measured were consistent with other data found in this study, particularly the Gaussian mixture modeling results (Fig. 4). Ex vivo samples displayed

a larger average mucus complex size and greater overall surface coverage than in vitro samples. This suggested that the ex vivo samples form larger gel matrixes and that more mucus was present in these samples. It is worth noting that this could potentially be caused by a larger cell presence within the ex vivo samples, with nearly 40-fold more cells per image (detected via DNA staining) in these samples compared with images of the same size of in vitro samples (Fig. 7 e). Also, the large variability in average complex size in the ex vivo samples was consistent with the hypothesis that mucus in those samples was more heterogeneous than the diffuse mucus layer in in vitro samples. This observation is in keeping with previous results showing high variability in mucus complex size in native samples of lung mucus compared with mucus collected from in vitro lung cell culture (42). Overall, these results provide evidence that the mucus formed in ALI in vitro culture is of similar composition but different structure than harvested native mucus.

CONCLUSIONS

In summary, we utilized a VIP-assisted ALI culture of primary human colonic epithelial cells to generate a thick,

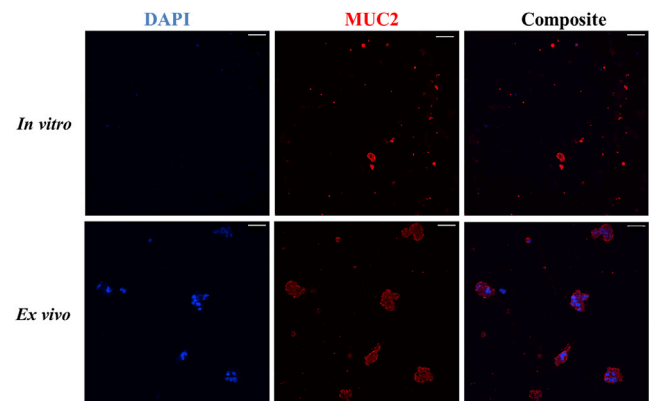


FIGURE 6 Staining of DNA and MUC2 in in vitro and ex vivo samples. Confocal microscopy images were acquired of the in vitro apical washings and ex vivo mucosal scrapings after staining DNA (blue) and MUC2 (red). Scale bar in all images represents 50 μm .

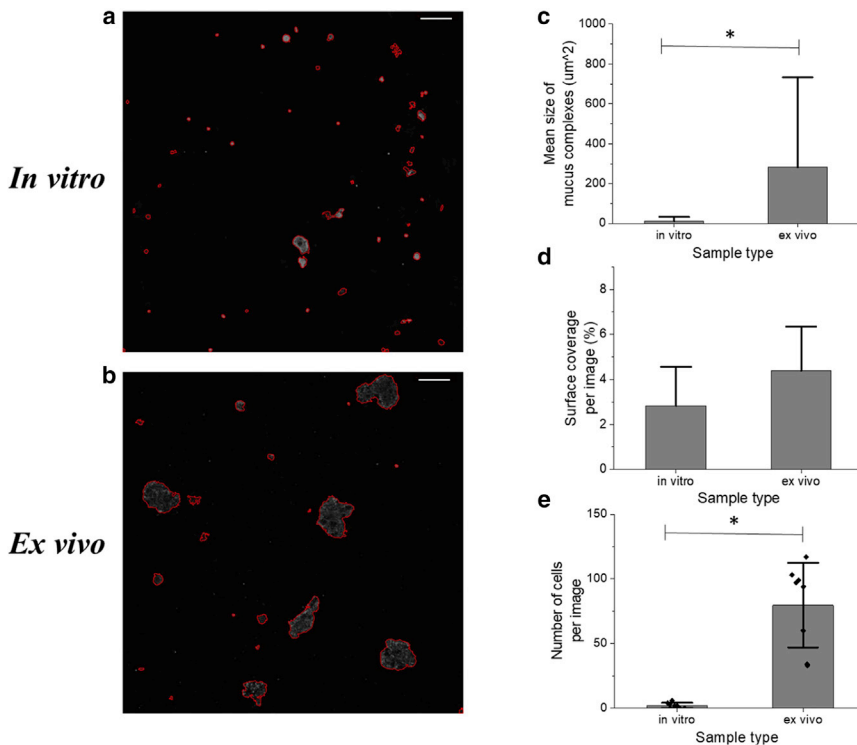


FIGURE 7 Quantifying the complex size and surface coverage of in vivo and ex vivo. DNA and MUC2 in mucus complexes were stained and their size quantified. Representative images of this result are shown for both in vitro (a) and ex vivo (b) samples. The mean size of these complexes in μm^2 was calculated (c), and the average surface coverage of mucus over the entire image relative to the background was calculated (d). The number of cells in each image included in this data set was also calculated from the presence of DNA clusters within each image (e). Scale bar for all images is $50 \mu\text{m}$. Statistical significance was detected in 7C and 7D ($p < 0.01$ for each) but not in 7E ($p = 0.13$).

contiguous mucus layer that could be harvested in sufficient quantities for measurement of macro- and microbiobiochemical and biophysical attributes. As the duration of cell culture or mucus formation lengthened, the percent solids within the mucus increased suggesting that the mucus matured over time. The macro- and microrheological properties of the in-vitro-formed mucus were compared with that of ex vivo and mucus samples collected from surgical specimens. On the macroscale, ex vivo mucus displayed stronger mechanical properties than the in vitro mucus with a larger G' and η^* . Additionally, in vitro mucus displayed a measurable power-law relation between the percentage of solids in the sample and the viscoelastic moduli. On the microscale, once heterogeneity was accounted for, there was no significant difference in rheological properties between the ex vivo and in vitro samples. The ex vivo samples demonstrated a greater degree of heterogeneity in composition relative to the in vitro samples, likely due to intermixing of cell debris with the ex vivo mucus. In contrast, the in vitro samples formed a looser mucus network relative the ex vivo mucus because of the absence of contaminating cellular material. This hypothesis was supported by the larger molar mass and radius of gyration of the ex vivo mucins relative to the in vitro samples. Finally, measurement of mucus particle size demonstrated physically larger mucin complexes in the ex vivo samples compared with the in vitro samples. Although not identical, the in vitro mucus was remarkably similar in the measured biophysical properties and biochemical attributes to that of ex vivo mucus. The VIP-assisted

ALI culture of primary colonic epithelium is a powerful model system for both the harvest of human intestinal mucus and the study of its rheological behavior and biochemical properties. Now that the relevance of the culture system has been validated, it could be used for a number of potential experimental pathways in the future. Of particular interest would be generating mucus with in vitro crypts, rather than monolayers, to increase physiological relevance; also of interest would be bacterial coculture, as well as analysis of the distribution of mucin types within the collected samples. Although the system as it stands does not produce mucus identical to native mucus, it is more successful than other systems at providing a high volume of mucus with similar physical properties to native mucus for substantial biophysical analysis. As such, it provides a useful tool for future studies of colonic mucus.

AUTHOR CONTRIBUTIONS

R.L.H., N.L.A., D.B.H., and C.E. designed experiments. R.L.H., C.E., M.M., and Y.W. performed experiments. S.S. provided technical support. R.L.H., M.M., C.E., and D.B.H. analyzed data. All authors took part in writing the manuscript.

ACKNOWLEDGMENTS

The authors thank Scott Magness for providing human colonic epithelial tissue, Kenza Araba for assistance in mucus staining, and Matthew Schaner and Shehzad Sheikh for assistance in native tissue collection. The authors

also thank Lawrence Bacudio and William Kissner for assistance in rheological measurements.

This work was supported by the National Institutes of Health, National Institute of Diabetes and Digestive and Kidney Diseases award DK120606 (to N.L.A. and Y.W.), 1R01DK104828-01A1 (to S.Z.S) and P30 DK065988 (to D.B.H., R.L.H., and C.E.), the National Science Foundation GRFP (Graduate Research Fellowship Program) Grant #2016212411 (to R.L.H.), and the following Cystic Fibrosis Foundation awards: HILL19GO (to D.B.H.), BOUCHE19XX0 (to D.B.H. and R.L.H.), and HILL20Y2-OUT (to D.B.H. and M.M). Also supported by Helmsley Charitable Trust Sinai-Helmsley Alliance for Research Excellence (SHARE) Project #2 (to S.Z.S). These authors disclose the following items: Y.W. and N.L.A. have a financial interest in Altis Biosystems. The remaining authors disclose no conflicts.

REFERENCES

- Allison, P. R., and A. S. Johnstone. 1953. The oesophagus lined with gastric mucous membrane. *Thorax*. 8:87–101.
- Singh, P. K., M. R. Parsek, ..., M. J. Welsh. 2002. A component of innate immunity prevents bacterial biofilm development. *Nature*. 417:552–555.
- Hodges, R. R., and D. A. Dartt. 2010. Conjunctival goblet cells. In *Encyclopedia of the Eye*. Academic Press, pp. 369–376.
- Johansson, M. E. V., H. Sjövall, and G. C. Hansson. 2013. The gastrointestinal mucus system in health and disease. *Nat. Rev. Gastroenterol. Hepatol.* 10:352–361.
- Hattrup, C. L., and S. J. Gendler. 2008. Structure and function of the cell surface (tethered) mucins. *Annu. Rev. Physiol.* 70:431–457.
- Johansson, M. E. V. 2012. Fast renewal of the distal colonic mucus layers by the surface goblet cells as measured by in vivo labeling of mucin glycoproteins. *PLoS One*. 7:e41009.
- Audie, J. P., A. Janin, ..., J. P. Aubert. 1993. Expression of human mucin genes in respiratory, digestive, and reproductive tracts ascertained by in situ hybridization. *J. Histochem. Cytochem.* 41:1479–1485.
- Atuma, C., V. Strugala, ..., L. Holm. 2001. The adherent gastrointestinal mucus gel layer: thickness and physical state in vivo. *Am. J. Physiol. Gastrointest. Liver Physiol.* 280:G922–G929.
- Gum, J. R., Jr., J. W. Hicks, ..., Y. S. Kim. 1994. Molecular cloning of human intestinal mucin (MUC2) cDNA. Identification of the amino terminus and overall sequence similarity to prepro-von Willebrand factor. *J. Biol. Chem.* 269:2440–2446.
- Ambort, D., M. E. V. Johansson, ..., G. C. Hansson. 2012. Calcium and pH-dependent packing and release of the gel-forming MUC2 mucin. *Proc. Natl. Acad. Sci. USA*. 109:5645–5650.
- Schroeder, B. O. 2019. Fight them or feed them: how the intestinal mucus layer manages the gut microbiota. *Gastroenterol. Rep. (Oxf.)*. 7:3–12.
- Johansson, M. E. V., J. M. H. Larsson, and G. C. Hansson. 2011. The two mucus layers of colon are organized by the MUC2 mucin, whereas the outer layer is a legislator of host-microbial interactions. *Proc. Natl. Acad. Sci. USA*. 108 (Suppl 1):4659–4665.
- Kamphuis, J. B. J., M. Mercier-Bonin, ..., V. Theodorou. 2017. Mucus organisation is shaped by colonic content; a new view. *Sci. Rep.* 7:8527.
- Clevers, H. 2013. The intestinal crypt, a prototype stem cell compartment. *Cell*. 154:274–284.
- Coglitore, D., S. P. Edwardson, ..., M. Whelan. 2017. Transition from fractional to classical Stokes-Einstein behaviour in simple fluids. *R. Soc. Open Sci.* 4:170507.
- Wang, Y., R. Kim, ..., N. L. Allbritton. 2017. formation of human colonic crypt array by application of chemical gradients across a shaped epithelial monolayer. *Cell. Mol. Gastroenterol. Hepatol.* 5:113–130.
- Sontheimer-Phelps, A., D. B. Chou, ..., D. E. Ingber. 2020. Human colon-on-a-chip enables continuous in vitro analysis of colon mucus layer accumulation and physiology. *Cell. Mol. Gastroenterol. Hepatol.* 9:507–526.
- Sardelli, L., D. P. Pacheco, ..., P. Petrini. 2019. Towards bioinspired in vitro models of intestinal mucus. *RSC Advances*. 9:15887–15899.
- Webber, S. E., and J. G. Widdicombe. 1987. The effect of vasoactive intestinal peptide on smooth muscle tone and mucus secretion from the ferret trachea. *Br. J. Pharmacol.* 91:139–148.
- Kesimer, M., S. Kirkham, ..., J. K. Sheehan. 2009. Tracheobronchial air-liquid interface cell culture: a model for innate mucosal defense of the upper airways? *Am. J. Physiol. Lung Cell. Mol. Physiol.* 296:L92–L100.
- Wang, Y., R. Kim, ..., N. L. Allbritton. 2019. Building a thick mucus hydrogel layer to improve the physiological relevance of in vitro primary colonic epithelial models. *Cell. Mol. Gastroenterol. Hepatol.* 8:653–655.e5.
- Hill, D. B., and B. Button. 2012. Establishment of respiratory air-liquid interface cultures and their use in studying mucin production, secretion, and function. In *Mucins: Methods and Protocols*, Methods in Molecular Biology. M. A. McGucki and D. J. Thornton, eds. Humana Press, pp. 245–258.
- Wang, Y., M. DiSalvo, ..., N. L. Allbritton. 2017. Self-renewing monolayer of primary colonic or rectal epithelial cells. *Cell. Mol. Gastroenterol. Hepatol.* 4:165–182.e7.
- Mason, T. G. 2000. Estimating the viscoelastic moduli of complex fluids using the generalized Stokes-Einstein equation. *Rheol. Acta*. 39:371–378.
- Hill, D. B., P. A. Vasquez, ..., M. G. Forest. 2014. A biophysical basis for mucus solids concentration as a candidate biomarker for airways disease. *PLoS One*. 9:e87681.
- Gardel, M. L., M. T. Valentine, and D. A. Weitz. 2005. Microrheology. In *Microscale Diagnostic Techniques*. K. S. Breuer, ed. Springer, pp. 1–49.
- Wang, Y., R. Kim, ..., N. L. Allbritton. 2018. Analysis of interleukin 8 secretion by a stem-cell-derived human-intestinal-epithelial-monolayer platform. *Anal. Chem.* 90:11523–11530.
- Allen, A., and G. Flemström. 2005. Gastroduodenal mucus bicarbonate barrier: protection against acid and pepsin. *Am. J. Physiol. Cell Physiol.* 288:C1–C19.
- Yuan, S., M. Hollinger, ..., J. V. Fahy. 2015. Oxidation increases mucin polymer cross-links to stiffen airway mucus gels. *Sci. Transl. Med.* 7:276ra27.
- Okumura, R., and K. Takeda. 2017. Roles of intestinal epithelial cells in the maintenance of gut homeostasis. *Exp. Mol. Med.* 49:e338.
- Celli, B. R., and P. J. Barnes. 2007. Exacerbations of chronic obstructive pulmonary disease. *Eur. Respir. J.* 29:1224–1238.
- Thim, L., F. Madsen, and S. S. Poulsen. 2002. Effect of trefoil factors on the viscoelastic properties of mucus gels. *Eur. J. Clin. Invest.* 32:519–527.
- Erickson, A. M., B. I. Henry, ..., C. N. Angstrom. 2015. Predicting first traversal times for virions and nanoparticles in mucus with slowed diffusion. *Biophys. J.* 109:164–172.
- Button, B., L.-H. Cai, ..., M. Rubinstein. 2012. A periciliary brush promotes the lung health by separating the mucus layer from airway epithelia. *Science*. 337:937–941.
- Yakubov, G. E., A. Papagiannopoulos, ..., T. A. Waigh. 2007. Molecular structure and rheological properties of short-side-chain heavily glycosylated porcine stomach mucin. *Biomacromolecules*. 8:3467–3477.
- Shchipunov, Y., S. Sarin, ..., C.-S. Ha. 2010. Hydrogels formed through regulated self-organization of gradually charging chitosan in solution of xanthan. *Green Chem.* 12:1187–1195.
- Lai, S. K., Y.-Y. Wang, ..., J. Hanes. 2009. Micro- and macrorheology of mucus. *Adv. Drug Deliv. Rev.* 61:86–100.

38. Serisier, D. J., M. P. Carroll, ..., S. A. Young. 2009. Macrorheology of cystic fibrosis, chronic obstructive pulmonary disease & normal sputum. *Respir. Res.* 10:63.
39. Mellnik, J., P. A. Vasquez, ..., M. G. Forest. 2014. Micro-heterogeneity metrics for diffusion in soft matter. *Soft Matter*. 10:7781–7796.
40. Esther, C. R., Jr., M. S. Muhlebach, ..., R. C. Boucher. 2019. Mucus accumulation in the lungs precedes structural changes and infection in children with cystic fibrosis. *Sci. Transl. Med.* 11:eaav3488.
41. Hill, D. B., R. F. Long, ..., B. Button. 2018. Pathological mucus and impaired mucus clearance in cystic fibrosis patients result from increased concentration, not altered pH. *Eur. Respir. J.* 52:1801297.
42. Markovetz, M. R., D. B. Subramani, ..., D. B. Hill. 2019. Endotracheal tube mucus as a source of airway mucus for rheological study. *Am. J. Physiol. Lung Cell. Mol. Physiol.* 317:L498–L509.